

Performances of the LHAASO detectors

Mingjun Chen,^{a,c} Huihai He,^{a,b,c,*} Chao Hou,^{a,c} Shoushan Zhang^{a,c} and Xiong Zuo^{a,c} for the LHAASO collaboration

^aKey Laboratory of Particle Astrophysics, Institute of High Energy Physics, Chinese Academy of Sciences, 100049 Beijing, China

^bUniversity of Chinese Academy of Sciences, 100049 Beijing, China

^cTIANFU Cosmic Ray Research Center, Chengdu, Sichuan, China

E-mail: mjchen@ihep.ac.cn, [hhh@ihep.ac.cn](mailto:h hh@ihep.ac.cn), houc@ihep.ac.cn,
zhangss@ihep.ac.cn, zuoxiong@ihep.ac.cn

The Large High Altitude Air Shower Observatory (LHAASO) is a new generation hybrid cosmic ray observatory which aims to explore the mystery of the origin of cosmic rays. It consists of one-kilometer square array (KM2A) with 5216 electromagnetic particle detectors and 1188 muon detectors, a water Cherenkov detector array (WCDA) with 3120 cells, a wide field-of-view air Cherenkov telescope array (WFCTA) with 18 telescopes. Physical data taking started in 2019 with one-quarter of the detectors in operation. The portion of detectors in operation increased with time going on. In 2021, the full array was put into scientific operation. The performances of the LHAASO detectors are presented.

38th International Cosmic Ray Conference (ICRC2023)
26 July - 3 August, 2023
Nagoya, Japan



*Speaker

1. Introduction

The Large High Altitude Air Shower Observatory (LHAASO) [1] is a hybrid extensive air shower (EAS) array with an area of 1.3 km^2 at an altitude of 4,410 m a.s.l. in Sichuan province, China, aiming for very high energy gamma ray astronomy and cosmic ray physics around the spectrum knees. It consists of one-kilometer square array (KM2A) with 5216 electromagnetic particle detectors (EDs) and 1188 muon detectors (MDs), a water Cherenkov detector array (WCDA) with 3120 units, a wide field-of-view air Cherenkov telescope array (WFCTA) with 18 telescopes. Physical data taking started in 2019 with one-quarter of the detectors in operation. The portion of detectors in operation increased with time going on. In 2021, the full array was put into scientific operation.

2. The electromagnetic particle detectors (EDs)

An ED is designed to measure the density and arrival times of EAS secondary particles (including e^\pm , γ , μ^\pm , etc.). The detection efficiency of an ED to minimum ionization particles (MIPs) is required to be $> 95\%$, with a time resolution of better than 2 ns and a signal charge resolution of $< 25\%$ (defined as the sigma/mean of the signal charge distribution). The dynamic range for each ED is designed to be from 1 to 10^4 particles, with the upper limit corresponding to the large number of EAS secondaries near the shower core of primaries with energy up to 100 PeV [2] [3].

The stability of the single-particle response is an important parameter to monitor the detector performances (e.g., light yield, PMT gain, signal amplification, etc.) and its degradation through the lifetime. The most probable value (MPV) of MIP charge spectrum provides an estimation of the output charge corresponding to a single-particle [4]. As an example, the single particle signal charge spectrum of one ED during 4 hours of data taking is shown in Fig. 1, together with the MPV of the single particle spectrum of three EDs from January 2022 to December 2022.

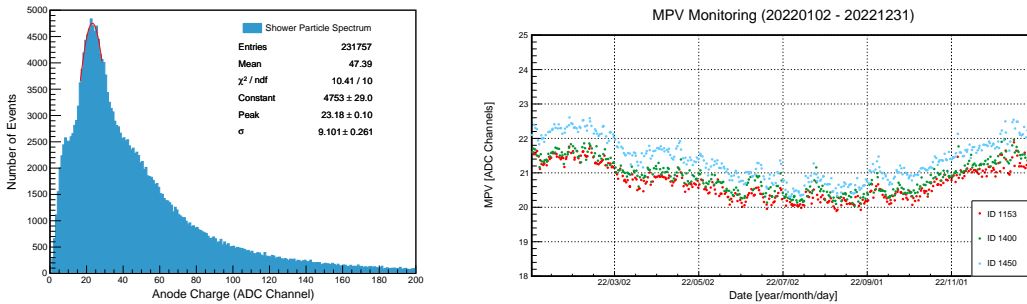


Figure 1: Left: an example of a shower particle spectrum in ADC channel units for one ED (ID 998). Fitting this distribution with a Gaussian yields a peak value of 23.18 ± 0.10 ADC channels/MIP. Right: Variation of the shower particle spectrum peak of three EDs (ID 1153, 1400 and 1450) from January 2022 to December 2022.

Keeping all the EDs time synchronized is critical for optimal pointing accuracy and angular resolution of the ED array. To calibrate the relative time offsets among the numerous detector units

in the EAS array, an offline calibration technique is applied [5], which also provides an ideal method to monitor the detector timing performance during its exposure. Figure.2-left shows the distribution of time offsets for all EDs under operation on October 10, 2022. Some EDs have parameters that are higher than those of the majority because the PMTs in these EDs have 10 dynode stages thus larger transition time. During the operation, the time calibration is carried out once everyday. The variation of the time offsets of five EDs from January 2022 to December 2022 is shown in Figure.2-right. The detector time offsets remains stable and vary less than 0.5 ns in one year.

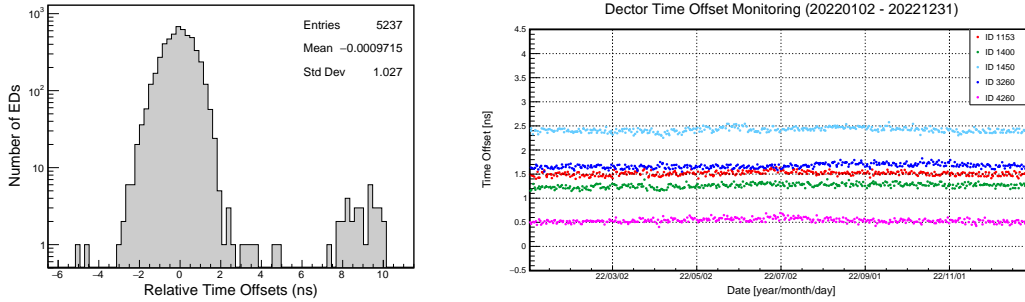


Figure 2: Left: distribution of time calibration parameters for all EDs under operation on October 10, 2022. Right: Variation of the relative time offsets of five EDs (ID 1153, 1400, 1450, 3260 and 4260) from January 2022 to December 2022.

3. The muon detectors (MDs)

An MD is a water Cherenkov detector enclosed within a cylindrical concrete tank with an inner diameter of 6.8 m and height of 1.2 m. An 8-inch PMT is installed at the top center of the tank to collect the Cherenkov light produced by high energy particles as they pass through the water. The whole detector is covered by a steel lid underneath soil. The thickness of the overburden soil is 2.5 m, to absorb the secondary electrons/positrons and γ -rays in showers. Thus the particles that can reach the water inside and produce Cherenkov signals are almost exclusively muons, except for those MDs located at the very central part of showers where some very high energy EM components may have a chance to punch through the screening soil layer. The detection efficiency of a typical MD to muons is 95%. The time resolution of an MD is about 10 ns. The charge resolution of the particle counter is 25% for a single muon and the dynamic range is from 1 to 10^4 particles. The average single rate of an MD is about 8 kHz with a threshold equivalent to 0.4 particles at the LHAASO site.

The vertical equivalent muon (VEM) is selected as the basis of charge calibration. The VEMs for all MDs in the array is shown in Figure.3-left. These two peaks corresponds respectively to single-layer and double-layer Tyvek liners used in the water bags of the muon detectors.

Figure.3-right shows the monitoring of normalized number of photoelectrons of single muon signals measured by a typical muon detector. A decrease of less than 2% is observed within 4 years.

The signal charge resolution for single muons is defined as the ratio of sigma to mean of the VEM of an MD. The charge resolutions for all MDs have been shown in Figure.4 All the MD

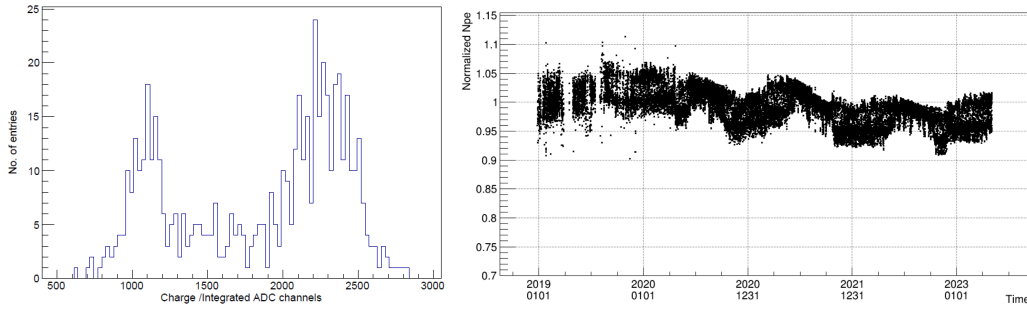


Figure 3: VEMs of all muon detectors (left) and normalized NPE of single muon signals varying with time (right).

possess fairly good signal charge resolution $< 25\%$ except a few detectors with single layer of Tyvek liner for water bag.

The MD time resolution is measured from the distribution of the MD time residual to shower fronts. The shower direction is measured by the EAS array with EDs. The detector time resolution is defined as the ratio of FWHM (full width at half maximum) over 2.35. The time resolutions for all MDs is shown in Figure.4-right, most of the time resolution is less than 8 ns , only 1 out of 1184 exceeds 10 ns .

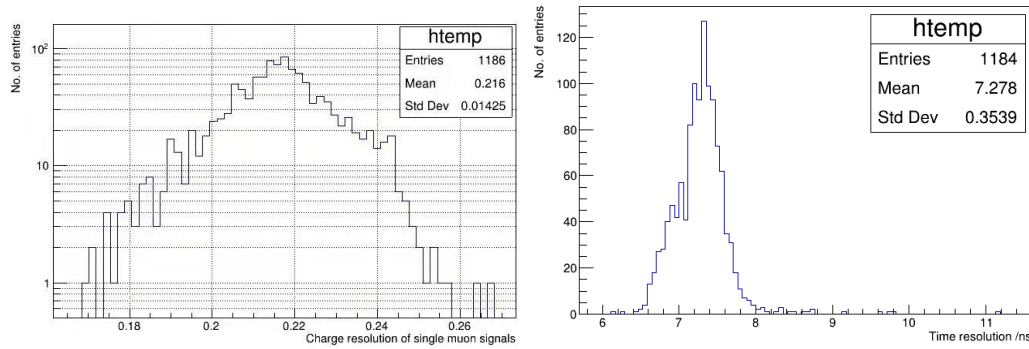


Figure 4: Charge (left) and time (right) resolutions of all muon detectors.

4. The water Cherenkov detectors

The main purpose of the water Cherenkov detector array (WCDA) [1] is to achieve a survey of gamma ray sources throughout the northern sky in the very high energy (100 GeV-30 TeV) region, and discovering a large number of gamma-ray sources. WCDA, covering an area of about $78,000\text{ m}^2$, is constituted by 3,120 detector units divided into 3 separate pools. Each pool is filled with clean water with 4.4 meters depth, two of them with an effective area of $150 \times 150\text{ m}^2$ contain 900 detector units each, and the third pool with an area of $300 \times 110\text{ m}^2$ contains 1,320 detector units. Each detector unit has a $5 \times 5\text{ m}^2$ area divided by black plastic curtains vertically hung in the water to screen the scattered light.

In each detector unit, a large and a small PMT are arranged. The large PMT (8-inch in pool 1 and 20-inch in pool 2 and 3) measures the number of photons and its arrival time. The 20-inch

PMT [6][7] enhances the gamma ray detecting sensitivity at energies below 500 GeV. Figure 5-left shows the charge spectrum of an 8-inch PMT and a 20-inch PMT. Here, three peaks [8] are clearly observed in 8-inch PMT’s spectrum. The first peak comes from the single photo-electron signals thus can be used to monitor the gain variation of the PMT and the stability of the detector system. The second peak, which is formed by geometrical effect of cosmic muons, is used to monitor and measure water transparency. The third peak originates from cosmic muons directly hitting the photo-cathode, which acts as a charge calibration parameter. As to the 20-inch PMTs’, the third peak is not complete due to the limitation of dynamic range. To enlarge the dynamic range of the detector, a small PMT (1.5-inch or 3-inch) is deployed beside the large PMT in each cell, which is designed to make precise measurements in shower core to identify the composition of cosmic ray events from 100 TeV to a few PeV. Figure 5-right shows the long-term stability of the first peak position of the charge spectrum of three large PMTs from three pools, respectively, and the variation of ADC counts is near 2%.

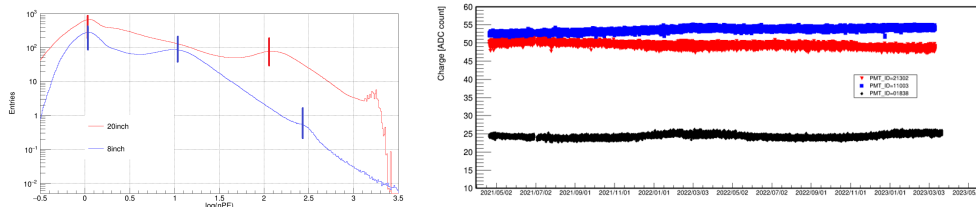


Figure 5: Left: the charge spectrum of an 8-inch PMT and a 20-inch PMT. The vertical lines mark the peaks; right: Long-term stability graph of the first peak position of the charge spectrum of three large PMTs. Black dots are from one 8-inch PMT, the other color points are from two 20-inch PMTs.

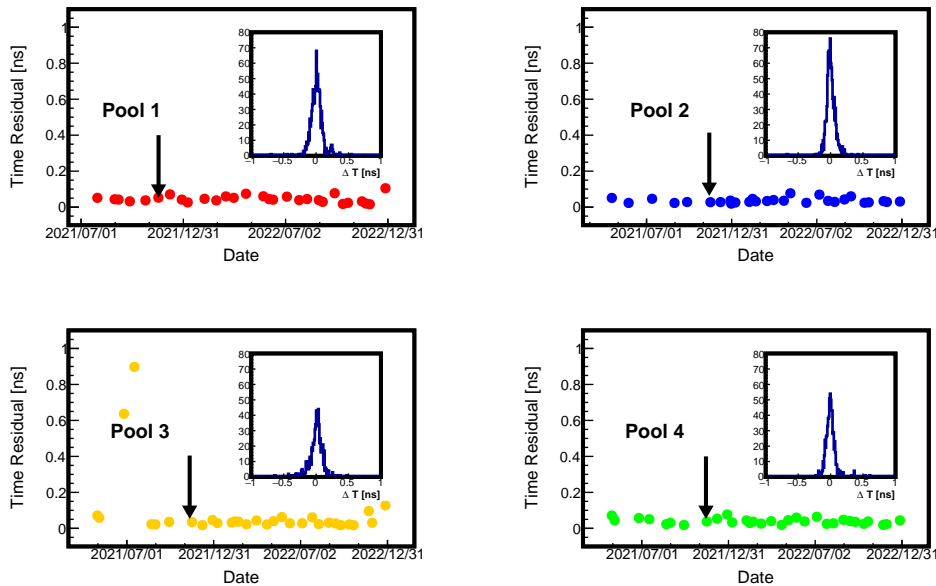


Figure 6: Long-term stability of the time calibration system.

The precision of the time measurement for the shower particles hitting every detector unit in

the array is directly related with the detection sensitivity for the sources. Therefore, we deployed a set of time calibration system[9] connecting each large PMT. Typically, one hour of calibration work is performed once a week. Figure 6 illustrates the good stability of the time calibration system for the entire detector in one and a half years, where the third pool is divided into two halves (the lower two graphs). Two points of the result of No.3 pool are a little large because of the clock jump of WR switch caused by a thunder in July, 2021. The small figure in the upper right corner is the results of one calibration, and all the values of sigma are smaller than 0.1 ns.

5. The wide field-of-view Cherenkov telescopes

WFCTA [10–12] consists of 18 wide-angle imaging air Cherenkov telescopes and each telescope has a field of view (FOV) of $16^\circ \times 16^\circ$ with a pixel size of approximately $0.5^\circ \times 0.5^\circ$. The main scientific goal of WFCTA is to measure the energy spectrum and composition of ultra-high energy cosmic rays (CRs) from dozens of TeV to a couple of EeV.

Each telescope consists of a 5 m^2 spherical reflector, a Silicon photomultiplier (SiPM) camera, a power supply system, a slow control system and an adjustable container. The camera is mounted at the focal plane of the reflector which is about 2870 mm from the camera. The container is mounted on a truck frame with a pitching rotation system that allows manually tilting it in the range of elevation angle from 0° to 90° with a step of 0.1° .

The camera [13] has 32×32 pixels grouped into 64 sub-clusters. On top of each sub-cluster is 4×4 square light funnels (Winston cone design) followed by 4×4 SiPMs. The funnel collects photons and focuses them on the SiPMs with a collection efficiency of about 90% for photons perpendicular to the entrance plane. The SiPM (Hamamatsu S14466) with photosensitive area of $15\text{ mm} \times 15\text{ mm}$ has about 359,424 Geiger-APD cells with a dynamic range of 3.5 decades in charge measurement.

The Night Sky Background (NSB) light significantly increases on moon nights, especially on full moon nights [13], thus the threshold value of each pixel is correspondingly increased to discriminate the signal from the noise. As a result, the event rate is modulated by the lunar phase as shown in Fig. 7. The event rate is almost unaffected by the moonlight at higher threshold, e.g. 200 PEs for single channel triggering and 3 pixels for adjacent pixel pattern recognition. From the simulation, the energy threshold is about 20 TeV on moonless nights, and about 50 TeV on full moon nights.

Six UV-LEDs with different wavelength (405 nm, 325 nm, 360 nm, 405 nm, 505 nm, 550 nm) are mounted at the center of the reflector [14] to monitor the gain of the camera. These LEDs are calibrated once a year by using a calibrated portable probe. The conversion factor from the FADC counts to the number of photons for each pixel in the camera was calibrated with an uncertainty less than 2.6% [14].

The moonlight can also induces a continuous photo-current in the SiPM, and leads to decrease of the bias voltage, so does the gain. On a clear and full moon night, when the moon is not in the telescope's field of view, the gain decreases less than 7% [13].

The stability of the camera gain are monitored when doors are closed, as shown in Fig. 8. The SiPM gain is stabilized within $\pm 2\%$ through a online high voltage and temperature compensation loop. The residual temperature effect can be corrected offline.

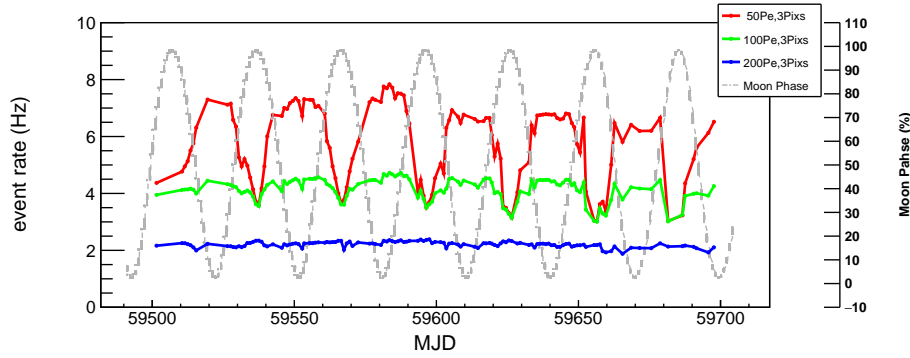


Figure 7: Event rates of a typical telescope at different offline thresholds during October 2021 - May 2022.

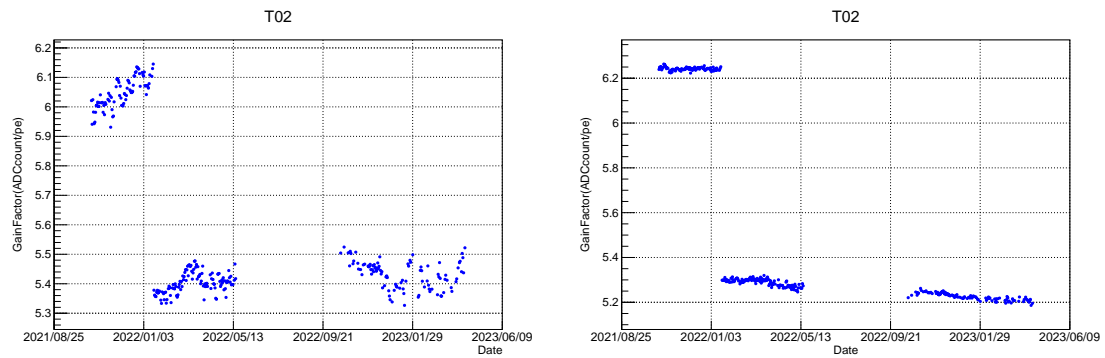


Figure 8: The camera gain before (left) and after (right) offline correction from October 2021 to April 2023 when doors are closed. On 18 January 2022, we adjusted the camera gain from about 6.1 to about 5.4. The left figure shows the online monitoring results.

6. Conclusions

The full array of LHAASO has been in stable operation for two years. All the LHAASO detectors are running smoothly with performances above the requirements. LHAASO has obtained and is expected to obtain a series of very important research results in both gamma ray astronomy and cosmic ray physics.

Acknowledgements

The authors would like to thank all staff members who work at high-altitude LHAASO site year-round to maintain the detector and keep the electrical power supply and other components of the experiment operating smoothly. We are grateful to the Chengdu Management Committee of Tianfu New Area for their consistent financial support of research with LHAASO data. This study was supported by the National Natural Science Foundation of China [Grant Nos. 12005246 and 12173039], the Department of Science and Technology of Sichuan Province [Grant No. 2021YFSY0030], the Key R&D Program of SiChuan Province [Grant No. 2019ZYZF0001], and the Xie Jialin Foundation of IHEP.

References

- [1] Zhen Cao et al. *The Large High Altitude Air Shower Observatory Science White Paper*, volume 46. Chinese Physics C, 2022.
- [2] H.H. He. Design of the LHAASO detectors. *Radiation Detection Technology and Methods*, 2:7, 2018.
- [3] F. Aharonian, Q. An, et al. Performance test of the electromagnetic particle detectors for the LHAASO experiment. *Nuclear Instruments and Methods in Physics Research Section A: Accelerators, Spectrometers, Detectors and Associated Equipment*, 1001:165193, 2021.
- [4] F. Aharonian, Q. An, et al. Self-calibration of lhaaso-km2a electromagnetic particle detectors using single particles within extensive air showers. *Phys. Rev. D*, 106:122004, Dec 2022.
- [5] H.K. Lv, H.H. He, et al. Calibration of the LHAASO-KM2A electromagnetic particle detectors using charged particles within the extensive air showers. *Astroparticle Physics*, 100:22–28, 2018.
- [6] Z. Cao et al. Upgrading plan towards multi-messenger observation with lhaaso. *RICAP*, 2019.
- [7] Mingjun Chen et al. Development of a magnetic shield for 20-inch microchannel plate photo-multiplier tubes. *Nuclear Instruments & Methods in physics research. Section A, Accelerators, spectrometers, detectors and associated equipment*, 1039:167128, 2022.
- [8] LHAASO Collaboration. Study on single-channel signals of water cherenkov detector array for the lhaaso project. *Nuclear Instruments & Methods in physics research. Section A, Accelerators, spectrometers, detectors and associated equipment*, 854:107–112, 2017.
- [9] J.Y. Liu et al. Test bench for fibers of the lhaaso-wcda time calibration system. *Journal of Instrumentation*, 12(10):P10021–P10021, 2017.
- [10] F. Aharonian et al. (The LHAASO Collaboration). Calibration of the air shower energy scale of the water and air cherenkov techniques in the lhaaso experiment. *Physical Review D*, 104:062007, 2021.
- [11] F. Aharonian et al. (The LHAASO Collaboration). Cosmic ray mass independent energy reconstruction method using cherenkov light and muon content in lhaaso. *Physical Review D*, page 043036, 2023.
- [12] F. Aharonian et al. (The LHAASO Collaboration). Reconstruction of cherenkov image by multiple telescopes of lhaaso-wfcta. *Radiation Detection Technology and Methods*, 6:544–557, 2022.
- [13] F. Aharonian et al. (The LHAASO Collaboration). Construction and on-site performance of the lhaaso wfcta camera. *Eur. Phys. J. C*, 81:657, 2021.
- [14] F. Aharonian et al. (The LHAASO Collaboration). Absolute calibration of lhaaso wfcta camera based on led. *Nucl. Inst. and Meth. A*, 1021:165824, 2022.